Temperature Dependence of the Nonequilibrium Kinetic Model That Describes the Adsorption and Desorption Behavior of CO2 in K-Promoted HTlc

ARTICLE *in* INDUSTRIAL & ENGINEERING CHEMISTRY RESEARCH · FEBRUARY 2010

Impact Factor: 2.59 · DOI: 10.1021/ie901210y

3 AUTHORS:

Hai du
Praxair Inc.
7 PUBLICATIONS **51** CITATIONS
SEE PROFILE

Armin Ebner
University of South Carolina
112 PUBLICATIONS **1,969** CITATIONS
SEE PROFILE

James A Ritter
University of South Carolina
132 PUBLICATIONS **2,055** CITATIONS
SEE PROFILE

Temperature Dependence of the Nonequilibrium Kinetic Model That Describes the Adsorption and Desorption Behavior of CO_2 in K-Promoted HTlc

Hai Du, Armin D. Ebner, and James A. Ritter*

Department of Chemical Engineering, University of South Carolina, Columbia, South Carolina 29208

A nonequilibrium kinetic model developed previously by the authors to describe the reversible adsorption and desorption behavior of CO_2 in a K-promoted hydrotalcite-like compound (HTlc) was extended to account for temperature effects. This model involves three steps and four phases that reversibly undergo adsorption or reaction with CO_2 in the structure. The model parameters were obtained by fitting it to experimental adsorption and desorption cycling data carried out with in-house-synthesized K-promoted HTlc at 11 temperatures ranging from 300 to 500 °C. A single adsorption (in CO_2 at 1 atm) and desorption (in He at 1 atm) cycle having a 700 min half-cycle time was obtained at each temperature and fitted successfully to the model. Then, using the same set of parameters, the model was used to successfully predict similar shorter cycle time experiments carried out with a 60 min half-cycle time for eight cycles at each temperature. For both the long and short cycle time data, the model captured all three kinetic regimes, the absolute CO_2 capacity, the CO_2 working capacity, the periodic behavior, and their temperature dependence. The deviations that did occur between the model and experiments were generally due to irreversible losses observed with the short cycle time runs at 480 and 500 °C that could not be predicted by the model; they were thus considered to be inconsequential. Both the model and experiments showed that temperature played an important role, with optimum temperatures being in the 380−420 °C range. Overall, this new model further validated that CO_2 uptake and release in K-promoted HTlc is associated with a combination of completely reversible adsorption, diffusion, and reaction phenomena, through a three-step, four-phase process that has a strong temperature dependence.

Introduction

Hydrotalcite-like compounds (HTlcs) have attracted considerable attention in the literature due to their reversible adsorption capacity for CO_2.[1–13] A K-promoted version of this material is being considered for the production of hydrogen by steam-methane reforming via the so-called sorption-enhanced reaction process (SERP).[4–9] It is also being considered for CO_2 capture from flue gas at elevated temperatures by pressure swing adsorption (PSA).[10–13]

From a mechanistic point of view, the reversible adsorption of CO_2 on HTlcs has been described as a high-temperature, diffusion-limited, equilibrium-driven process. Further, this phenomenon has been described as being akin to one or more physical or chemical adsorption processes.[2,3,10–15] Four different models have advanced this area of research.[2,14–17]

Ding and Alpay presented a simple Langmurian, physisorption representation of the equilibrium properties combined with a simple linear driving force (LDF) mass-transfer mechanism and with adsorption being about 10 times faster than desorption.[2] Ritter and co-workers made their equilibrium data temperature-dependent and used it for developing new PSA cycles for CO_2 capture.[10–12] However, the PSA cycles designed and conclusions drawn from those works might be incomplete, because the Ding and Alpay data were limited to a very narrow range of conditions with a low apparent heat of adsorption. Rodrigues and co-workers used a bi-Langmurian approach with one exothermic physisorption process and one endothermic chemisorption process to account for an observed maximum in the loading capacity with temperature. They accounted for mass-transfer effects through a Fickian or LDF diffusion process.[13,15] Ritter and co-workers developed a reversible, nonequilibrium, kinetic model that accounted for three observed rate processes: a fast mass-transfer-limited chemisorption process and two successively slower Langmuir−Hinshelwood kinetic processes.[16,17] Their third exceedingly slow process has recently been observed and discussed by others.[7–9] Sircar and co-workers also based their model on a Langmurian, chemisorption approach to account for an observed step change at high pressure in the adsorption isotherm that together represented a two-step mechanism.[14] An LDF approach was assumed for the mass-transfer process but with equal adsorption and desorption processes. Of those four models, only that by Ritter and co-workers was a nonequilibrium model and only their model provided a detailed mechanism that describes the equilibrium and kinetic behavior of CO_2 in K-promoted HTlc; however, their initial works were only done at one temperature, i.e., 400 °C.[16,17]

To further validate the dynamics and kinetics of the three reversible processes taking place during the uptake and release of CO_2 in K-promoted HTlc, and to provide a more useful version of the reversible nonequilibrium kinetic (RNEK) model for the proper design of a thermal swing adsorption (TSA) process, the objective of this article is to report on a temperature-dependent version of the RNEK model. This new version of the RNEK model now describes the reversible adsorption and desorption behavior of CO_2 on a K-promoted HTlc over a wide range of temperatures ranging from 300 to 500 °C. As such, it represents the most comprehensive and potentially most useful model in the literature of the four available,[2,14–17] as it potentially alleviates some of their limitations, as mentioned above, for example, in the design of PSA cycles.[10–12]

Mechanism and Temperature-Dependent RNEK Model Development. The mechanism depicted in Figure 1 was envisioned for the three reversible steps taking place during the uptake and release of CO_2 on K-promoted HTlc.[16,17] This was

* To whom correspondence should be addressed. Tel.: (803) 777-3590. Fax: (803) 777-8265. E-mail: ritter@cec.sc.edu.

10.1021/ie901210y
Published on Web 03/01/2010

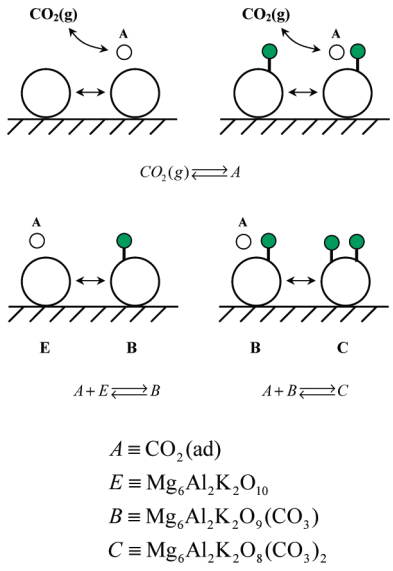

Figure 1. Pictorial representation of the proposed mechanism that describes the reversible adsorption and desorption behavior of CO_2 in K-promoted HTlc. No metal carbonate speciation is implied by the chemical formulas shown for phases E, B, and C.

not a trivial undertaking. The CO_2−HTlc system is not a simple one. Physical adsorption does not govern this process. Working capacities as large as 1 mol/kg simply do not occur by physical adsorption at 500 °C. Indeed, the true mechanism, of which no other researchers have attempted to describe, apart from the traditional LDF and Langmuir-like equilibrium process, must involve reactions of intricate nature. This RNEK model is simply a macroscopic approach that does not attempt to describe the microscopic nature of the process, but that nevertheless is able to predict the CO_2 behavior in a complex system.

In this way, the RNEK model was made simple enough to not involve too many parameters, but complex enough to capture the dynamics that other models failed to capture. Indeed, at least eight other models were evaluated systematically, as mentioned in ref 17, which painstakingly led to the current version of the RNEK model by adding just enough complexity step by step. This approach made it clear that an LDF plus equilibrium model, upon which all the other models in the literature are based, is simply unable to capture the long linear uptake trend that persists over several days.[7] Those equilibrium driven models simply cannot account for such behavior. This was one of the reasons why the RNEK model was developed.

The reaction pathway in the RNEK model involves three reversible reactions with slow, intermediate, and fast adsorption and desorption behavior, respectively. It also involves four phases that participate in these reactions, each one represented by a reaction site and denoted by letters A, B, C, and E. A possible chemical formulation for each of these phases is also given in Figure 1, with no implication toward identifying any of the metal carbonate species.[16,17]

An activation step occurs first and only once.[17] It is an irreversible step that transforms the inactive sites into active sites and consists of dehydration and dehydroxylation. During activation, reaction sites corresponding to phases C, B, and E are assumed to form and be present in the sample after activation. Phase C has two molecules of CO_2 strongly and chemically bound to the structure. Phase B has one molecule of CO_2 strongly and chemically bound to the structure and one empty site for binding CO_2. Phase E has two open sites for strongly and chemically binding CO_2 molecules to the structure. The CO_2 molecules in phases B and C are most likely in the form of carbonates, as depicted by Ebner et al.[17] These two sites combined represent the total number of strong reaction sites available for CO_2 binding. In contrast, phase A represents a site that weakly binds CO_2 through a chemisorption mechanism. Phase A can move freely within the structure and actively participate in the formation of both phases B and C. It is formed through a mass-transfer-limited process that results in the rapid conversion of gaseous CO_2 into chemisorbed CO_2.

According to the RNEK model, during adsorption, gaseous CO_2 molecules diffuse into the structure of the K-promoted HTlc and chemisorb to the sample to form weakly bound phase A through a fast mass-transfer process ($CO_2(g) \rightarrow A$). Then the uptake slows and the process becomes controlled by an adsorption/reaction sequence between diffusing phase A and empty phase E to form intermediate phase B ($A + E \rightarrow B$). Finally, the last pathway is dominated by an adsorption/reaction sequence between phases A and B to form CO_2 saturated phase C ($A + B \rightarrow C$). During desorption, CO_2 is first desorbed from phase A through the fast mass-transfer-limited process ($A \rightarrow CO_2(g)$). Then desorption slows, and the process becomes controlled by conversion of phase B into phases E and A by giving up one CO_2 molecule ($B \rightarrow A + E$). Finally, the desorption process is dominated by the slow conversion of phase C into phases A and B ($C \rightarrow A + B$).

On the basis of the above mechanism, the temperature-dependent analysis begins with the RNEK model developed by Ebner et al.[17] In this model three differential equations that represent the overall mass balances for the three reversible phases C, B, and A, and one algebraic equation that represents the mass balance restriction involving phases C, B, and E are written as

$$\frac{dq_C}{dt} = -k_{1,f}q_C + k_{1,b}q_Aq_B \tag{1}$$

$$\frac{dq_B}{dt} = k_{1,f}q_C - k_{1,b}q_Aq_B - k_{2,f}q_B + k_{2,b}q_Aq_E \tag{2}$$

$$\frac{dq_A}{dt} = k_m(q_{A,e} - q_A) + k_{1,f}q_C - k_{1,b}q_Aq_B + k_{2,f}q_B - k_{2,b}q_Aq_E \tag{3}$$

$$q_E \equiv q_T - q_B - q_C \tag{4}$$

The q's (except $q_{A,e}$) represent the site concentrations of each phase based on CO_2-free K-promoted HTlc (i.e., $Mg_6Al_2K_2O_{10}$).[17] $q_{A,e}$ represents the value of q_A in equilibrium at T and P_{CO_2}. Depending on whether the sample is undergoing adsorption or desorption, $q_{A,e}$ is defined differently. For adsorption, $q_{A,e,a}$ is defined according to

$$q_{A,e,a} = q_{A,max}\theta_{A,e,a}(P_{CO_2}) \tag{5}$$

$$q_{A,max} = \eta(q_B + 2q_E) \tag{6}$$

$$\eta = mn(T - T_o)/[1 + n(T - T_o)] \tag{7}$$

where $q_{A,max}$ is the maximum concentration of site A formed after activation. $\theta_{A,e,a}(P_{CO_2})$ is the fractional coverage of phase A in equilibrium with the partial pressure of CO_2. However, at the conditions investigated here it is assumed that $\theta_{A,e,a}$ is unity, as observed experimentally when the partial pressure of CO_2 is 1 atm or larger. η is a temperature-dependent parameter that physically represents the ratio between the actual and maximum number of reaction sites available. Equation 7 is the assumed temperature dependence of η, where m, n, and T_o are fitting

parameters and with η taking on values generally between 0 and 1. η is allowed to increase with temperature, which increases the number of actual reaction sites. The sum $q_B + 2q_E$ in eq 6 accounts for the number of sites available for A phase, i.e., one site for each B phase site and two sites for each E phase site. For desorption, $q_{A,e,d} = 0$, since the equilibrium condition for site A at the end of desorption is a vacant site, free of CO_2 molecules.

The k_m represents the mass-transfer coefficient for the process involving phase A and gaseous CO_2. In this mass-transfer process, a linear driving force (LDF) is defined between q_A and $q_{A,e}$. Also depending on whether the sample is undergoing adsorption or desorption, k_m is allowed to take on different values, as observed experimentally elsewhere:[2]

$$k_m = \begin{cases} k_{m,a} & q_{A,e} = q_{A,e,a} > q_A \\ k_{m,d} & q_{A,e} = q_{A,e,d} < q_A \end{cases} \quad (8)$$

Both k_m's, at least initially, are assumed to be temperature-dependent according to the following activated diffusion type expressions:

$$k_{m,a} = A_{m,a} \exp(-E_{m,a}/RT) \quad (9)$$

$$k_{m,d} = A_{m,d} \exp(-E_{m,d}/RT) \quad (10)$$

The k_1's and k_2's in eqs 1−3 represent the forward and backward reaction rate constants for the two reactions. These reaction constants are assumed, at least initially, to be temperature-dependent according to the following Arrhenius relationships:

$$k_{1,f} = A_{1,f} \exp(-E_{1,f}/RT) \quad (11)$$

$$k_{1,b} = A_{1,b} \exp(-E_{1,b}/RT) \quad (12)$$

$$k_{2,f} = A_{2,f} \exp(-E_{2,f}/RT) \quad (13)$$

$$k_{2,b} = A_{2,b} \exp(-E_{2,b}/RT) \quad (14)$$

Finally, the CO_2 loading q_T is defined in terms of q_A, q_B, and q_C, based on the CO_2 site occupancy of phases A−C just after activation. It is given by

$$q_{CO_2} \equiv (q_A - q_{A,o}) + (q_B - q_{B,o}) + 2(q_C - q_{C,o}) \quad (15)$$

This temperature-dependent RNEK model has 21 parameters. Values for five of these parameters (i.e., $\theta_{A,e,a}$, $q_{B,o}$, $q_{A,o}$, $q_{A,e,d}$, and q_T) are known a priori.[17] The remaining 16 parameters are fitting parameters. The methodology used to obtain of these parameters is explained below.

Material Preparation and Cycle Testing. An HTlc with molecular formula $[Mg_3Al(OH)_8]_2CO_3 \cdot nH_2O$ was prepared by a co-precipitation method.[1] While vigorously stirring, a solution of 41.7 mL of deionized water containing 0.75 mol of $Mg(NO_3)_2 \cdot 6H_2O$ and 0.25 mol of $Al(NO_3)_3 \cdot 9H_2O$ was added to a solution of 83.3 mL of deionized water containing 1.7 mol of NaOH and 0.5 mol of Na_2CO_3. The precipitate was separated from the slurry by vacuum filtration. The wet filter cake was washed with deionized water and vacuum-filtered three times, dried overnight at 60 °C in a vacuum oven, crushed, and calcined in air at 400 °C for 4 h.

A K-promoted HTlc with molecular formula $[Mg_3Al(OH)_8]_2CO_3 \cdot K_2CO_3 \cdot nH_2O$ was prepared using an incipient wetness procedure. To obtain an Al:K ratio of 1:1, a 0.33 M solution of K_2CO_3 was prepared in deionized water, and a predetermined volume of it was added to the HTlc powder in three steps: (1) The solution was added dropwise to the powder until it appeared wet. (2) The wet powder was dried for 15 min in a vacuum oven at 60 °C. (3) Steps 1 and 2 were repeated until all the solution was added.

A Perkin-Elmer TGA-7 thermogravimetric analyzer was used to measure the dynamic adsorption and desorption behavior of CO_2 on this K-promoted HTlc. A typical TGA run was carried out with a sample of K-promoted HTlc powder (~20 mg). This powder had a broad particle size distribution, with particle diameters ranging from 5 to 100 μm.

First, the sample was activated at 500 °C for 8 h in He flowing at around 60 cm^3/min and 1 atm. At the end of the activation step, the temperature was adjusted to a predetermined temperature between 300 and 500 °C using a 10 °C/min ramping rate. When the temperature was reached, the test gas was switched from He to CO_2 (also flowing at around 60 cm^3/min and 1 atm) to initiate adsorption and begin the first half of an adsorption−desorption cycle. This adsorption half-step was continued for a specified length of time, and then the gas was switched back to He to initiate desorption and finish the second half of the adsorption−desorption cycle. When the half-cycle time was set at a very long time of 700 min, one adsorption−desorption cycle was carried out to allow the system to approach equilibrium at the end of the adsorption and desorption steps. When the half-cycle time was set at a much shorter time of 60 min, eight adsorption−desorption cycles were carried to elucidate the dynamic behavior during cycling under more reasonable cycle times that were far away from equilibrium.

Results and Discussion

The definition of the CO_2 loading is introduced below, along with the content of all the figures. In the next section, the experimental results are explained. This is followed by a section that discusses how the model was calibrated (fitted) to the long cycle time experiments and the resulting predictions were obtained from that fitting procedure. The CO_2 loading presented in all the figures is in terms of a CO_2-free K-promoted HTlc, i.e., $Mg_6Al_2K_2O_{10}$. Due to the slow kinetics of desorption of K-promoted HTlc that limits the accurate determination of the mass of CO_2-free K-promoted HTlc, the CO_2 loading was estimated from the predicted loading at a reference state according to

$$q_{CO_2,exp} = \frac{w - w_o}{w_o} \frac{1}{M_{CO_2}} (1 + (q_{A,o} + q_{B,o} + 2q_{C,o}) M_{CO_2}) \quad (16)$$

where w represents the experimental mass obtained as a function of time during an experiment and w_o represents the value of w just after activation. This definition correctly allows the CO_2 loading to take on negative values, as explained later. Moreover, since the sample was not necessarily in an equilibrium state and slowly still losing weight at the end of the activation period, an activation time of 8 h was considered to be sufficient.

Figure 2a displays both experimental and modeling results for the long cycle time, 700 min adsorption and 700 min desorption cycle, run at 400 °C. Figure 2b displays both experimental and modeling results for the short cycle time, eight 60 min adsorption and 60 min desorption cycle runs at 400 °C. Parts c and d of Figure 2, respectively, show experimental and modeling results for the first 10 min of the adsorption and desorption steps shown in Figure 2a.

Figure 3 displays both experimental and modeling results for the long cycle time, single adsorption and desorption cycle at

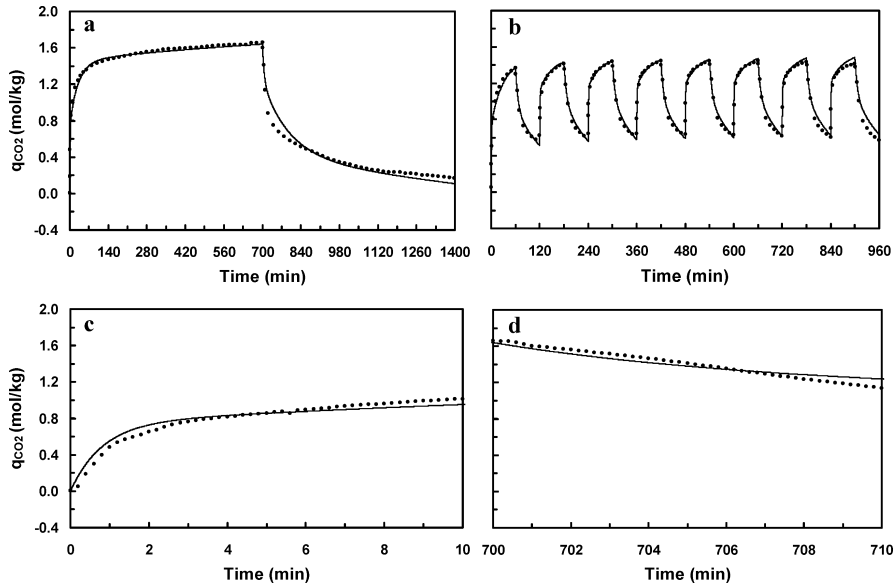

Figure 2. Experimental (symbols) and modeling (lines) results of the CO_2 loading in K-promoted HTlc at 400 °C for (a) a single adsorption (CO_2 at 1 atm) and desorption (He at 1 atm) cycle with a 700 min half-cycle time, (b) eight adsorption (CO_2 at 1 atm) and desorption (He at 1 atm) cycles with a 60 min half-cycle time, (c) first 10 min of the adsorption step in a; and d) first 10 min of the desorption step in a.

the 10 remaining temperatures ranging from 300 to 500 °C in 20 °C increments (excluding the 400 °C shown in Figure 2). Figure 4 displays the same information as in Figure 3, but for the short cycle time, eight adsorption and desorption cycle runs. Figure 5 plots the experimental and modeling results for the CO_2 loading obtained just at the end of the adsorption and desorption steps as a function of temperature for both the long cycle time runs (single cycle in Figure 3) and short cycle time runs (eighth cycle in Figure 4).

Long and Short Cycle Time Experiments. The results in Figure 2 are typical of the dynamic cycling experiments at all the other temperatures (shown later). Figure 2a shows the uptake and release of CO_2 was essentially reversible, an important finding for the use of K-promoted HTlc in a cyclic process. Figure 2b shows that periodic behavior was reached after just a few cycles, which implies K-promoted HTlc is quite stable in the presence of CO_2. Figure 2c shows how an equilibrium state could be mistakenly assumed after just 10 min or so of CO_2 uptake; however, the CO_2 loading nearly doubled after 700 min and was still increasing, which shows the futility of trying to reach a true equilibrium state in this system. Figure 2c also shows that the initial adsorption kinetics were relatively fast compared to the initial desorption kinetics shown in Figure 2d, an interesting finding with mechanistic implications that has also been observed by others.[7–9]

Figure 3 shows some interesting temperature effects with the long cycle time experiments. As the temperature increased, the following occurred: The initial adsorption and desorption kinetics tended to increase. The CO_2 uptake and release curves became increasingly more rectangular. The final CO_2 loading at the end of the adsorption step went through a maximum. The final CO_2 loading at the end of the desorption step kept decreasing, crossed the zero point, and even became negative. Since the loadings displayed in these figures were normalized to the weight of the sample at the end of the activation step (eq 16), as explained earlier, these negative CO_2 loadings simply indicated that more CO_2 was released over the 700 min half-cycle time desorption than that released during activation.

Figure 4 also shows some interesting temperature effects with the short cycle time experiments. As the temperature increased, the following occurred: The adsorption and desorption kinetics tended to increase, as observed from the sawtooth patterns becoming sharper. The overall CO_2 loading increased with the cycle number at the lower temperatures, leveled off at the intermediate temperatures, and decreased at the higher temperatures. Periodic behavior was approached at lower cycle numbers. It was also interesting that only for the 480 and 500 °C experiments the sawtooth patterns decreased in size after the first cycle, possibly indicating some irreversible losses in the CO_2 capacity occurred at these temperatures.

Some interesting temperature effects were also observed with the end of step CO_2 loadings in Figure 5. As the temperature increased, the following occurred: The CO_2 loading at the end of the adsorption step went through a maximum for both the long and short cycle time runs, but more so for the latter. In contrast, the CO_2 loading at the end of the desorption step decreased in a similar fashion for both the long and short cycle time runs. The corresponding CO_2 working capacity, i.e., the difference in the CO_2 loading at the end of the adsorption and desorption steps, increased with temperature for the long cycle time runs, and exhibited a slight maximum for the short cycle time runs perhaps due to the same irreversible behavior clearly observed in Figure 4 at 480 and 500 °C.

The long and short cycle time experimental results in Figures 2−5 collectively showed that CO_2 is completely reversible in K-promoted HTlc. They also showed that an optimum temperature exists for cycling CO_2 on and off this material. The best conditions seem to be in the 380−420 °C range. The 300 °C data exhibited very poor kinetics and a low CO_2 working capacity, while the 500 °C data exhibited some apparent irreversibility.

Model Calibration with Long Cycle Time Experimental Data. The temperature-dependent RNEK model is given by eqs 1−15. This model has 21 parameters. Five of these parameters (i.e., $\theta_{A,e,a}$, $q_{B,o}$, $q_{A,o}$, $q_{A,e,d}$, and q_T) were known a priori and obtained on the basis of the following constraints or assumptions.[17] $\theta_{A,e,a}$ was arbitrarily set equal to unity. q_T was a constant and calculated by assuming a stoichiometric carbonate capacity for the HTlc material. The equilibrium CO_2 loading in phase A at the end of desorption ($q_{A,e,d}$) was assumed to be zero. The initial CO_2 loading in phase A ($q_{A,o}$) and the same in phase B ($q_{B,o}$) were both assumed to be zero. Since all the samples were activated under the same conditions, $q_{C,o}$ was assumed to be a

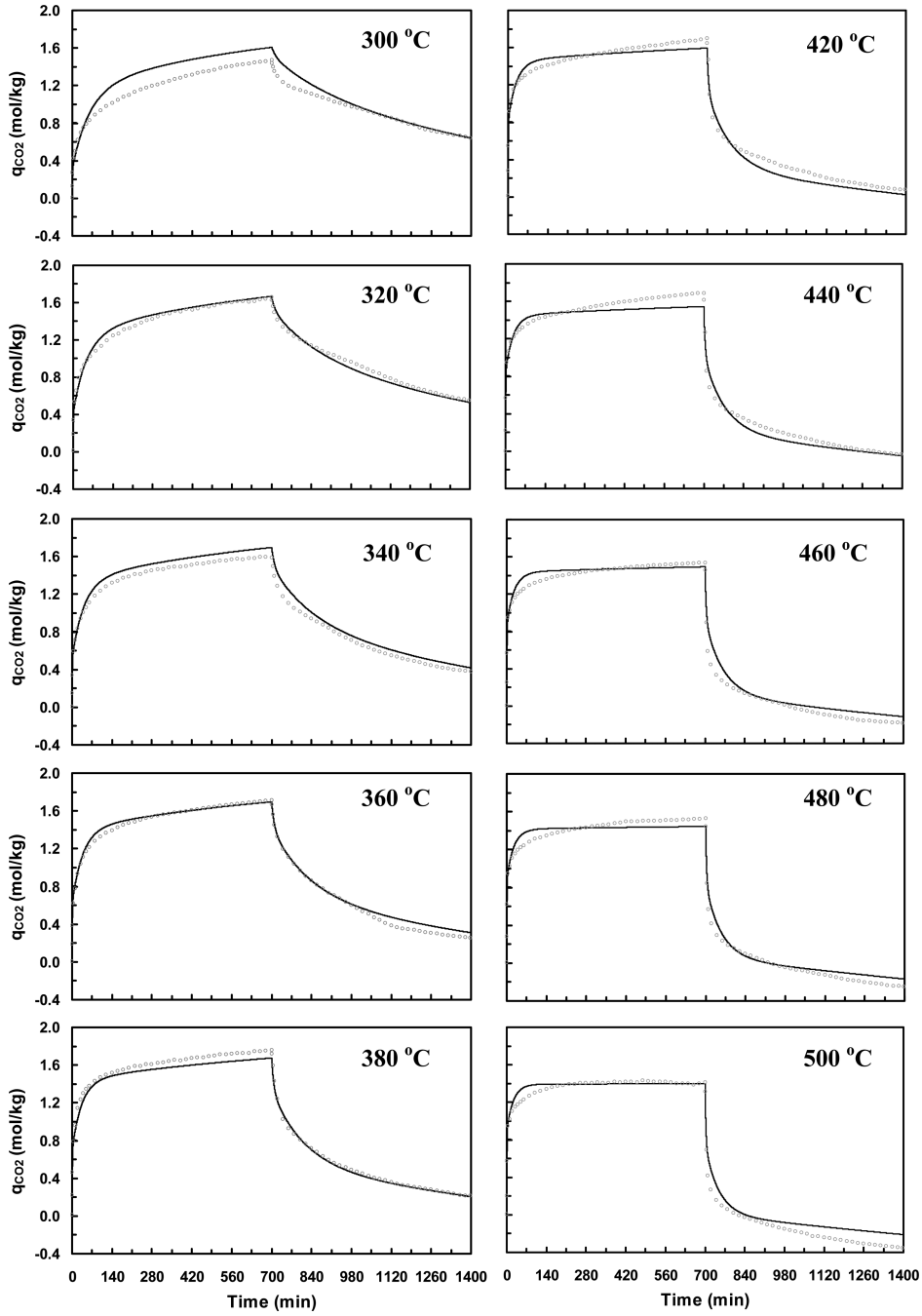

Figure 3. Experimental (symbols) and modeling (lines) results of the CO_2 loading in K-promoted HTlc from 300 to 500 °C in 20 °C increments for a single adsorption (CO_2 at 1 atm) and desorption (He at 1 atm) cycle with a 700 min half-cycle time.

constant and independent of temperature. The 16 remaining parameters were obtained as follows.

A systematic trial and error approach combined with nonlinear regression was utilized in lieu of more accurate statistical analysis and parameter estimation, because the focus was to only find a set of parameters which fit the experimental data over a wide range of conditions that are more suitable for adsorption process modeling. First, the long cycle time adsorption (700 min) and desorption (700 min) experimental results at 300 °C were fitted to the model. The resulting parameters were then used as the initial values to fit the long cycle time experiment at 320 °C; adjustments were made. This sequential approach was continued until the long cycle time experiment at 500 °C was fitted to the model. This individual fitting of all the long cycle time experiments at the different temperatures (300−500 °C) produced values of the reaction rate constants, mass-transfer coefficients, and η as a function of temperature. These values were plotted against temperature according to the respective relationships, and the above sequential fitting process was repeated until reasonable temperature relationships were obtained. Adjustments were made to the individual parameters as deemed appropriate using this trial and error/nonlinear regression approach to get the best fit of all the long cycle time experiments to the experimental data using just one set of model parameters. This set of temperature-independent model parameters is given in Table 1.

The results in Figures 2a,c,d, 3, and 5a collectively show that the model correlated very well with the long cycle time experimental data at all the temperatures. Parts a, c, and d of Figure 2 show that at 400 °C only minor deviations resulted for both the adsorption and desorption steps and for both the initial 10 min adsorption and desorption regimes. Although these

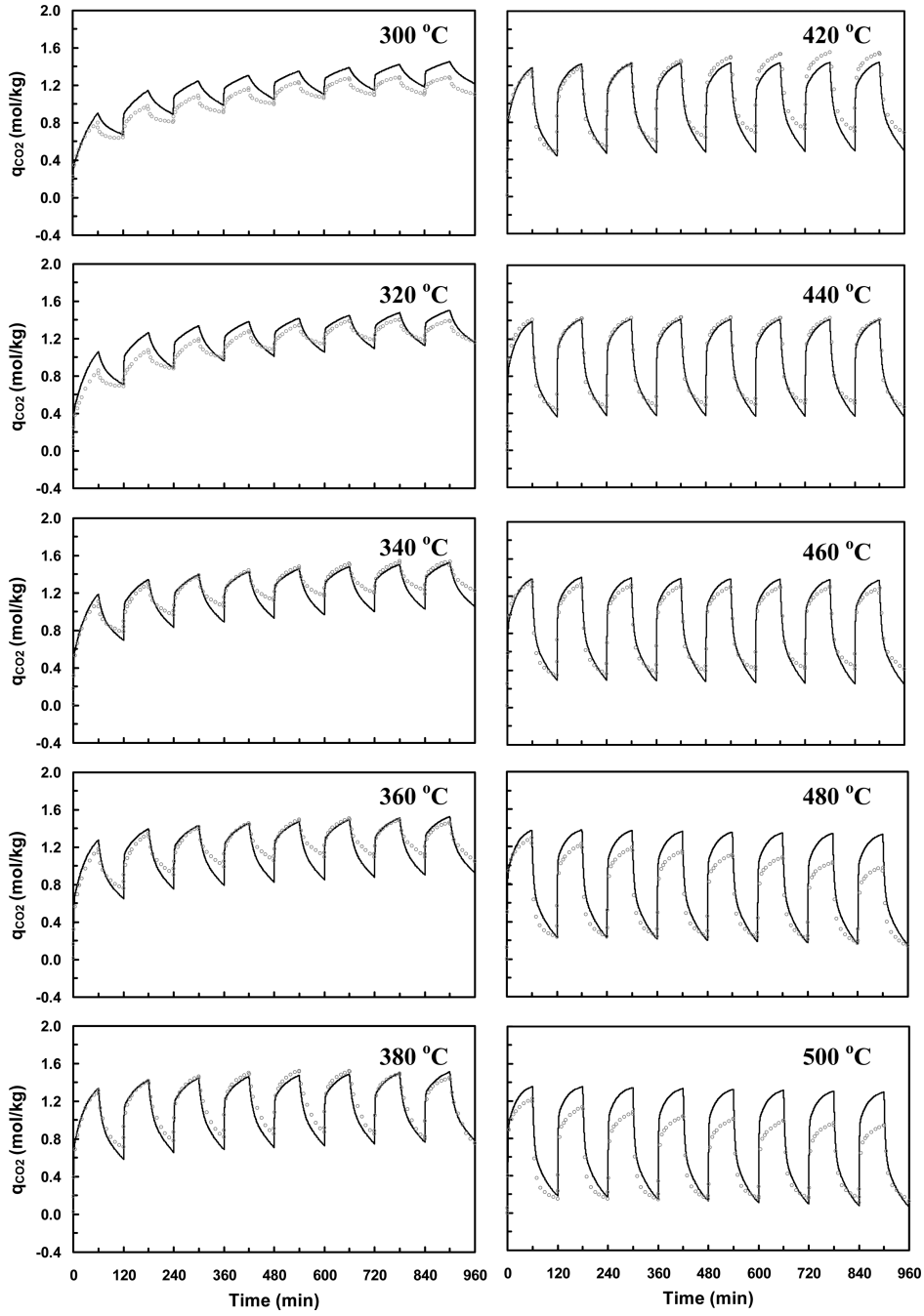

Figure 4. Experimental (symbols) and modeling (lines) results of the CO_2 loading in K-promoted HTlc from 300 to 500 °C in 20 °C increments for eight adsorption (CO_2 at 1 atm) and desorption (He at 1 atm) cycles with a 60 min half-cycle time.

very positive results were typical of most of the other temperatures, Figure 3 shows that somewhat larger deviations did occur at some of the other temperatures. These differences were considered to be inconsequential, however.

This very good agreement between the model and experiments over such a large temperature range lent some credence to the mechanism shown in Figure 1 that was developed by Ebner et al.[16,17] The magnitudes of the parameters obtained from the fitting exercise were also quite reasonable and generally realistic (Table 1). For example, the magnitudes of the adsorption (larger) and desorption (smaller) mass-transfer coefficients were generally in agreement with results reported by others,[2,4,11] and their order of magnitude difference was also observed by Ding and Alpay.[2] The values of the rate constants for the slowest reaction at different temperatures, i.e., $k_{1,f}$ and $k_{1,b,}$, substantiated that the reversible reaction of phase C into phases B and A was an extremely slow process that developed over a period of hundreds of hours. This result indicated that the sample might never reach a true equilibrium state. The model also substantiated that the reversible reaction of phase B into phases A and E, with parameters of $k_{2,f}$ and $k_{2,b}$, was an intermediate rate process, and that phase B could even disappear during desorption at the higher temperatures, as shown elsewhere.[16] This result verified the assumption made about $q_{B,o} = 0$ at the end of the activation period. The magnitudes and signs of the energy parameters also deserve some discussion.

As shown by eqs 9−14, activated diffusion and Arrhenius type functions were assumed for the temperature dependence of the adsorption and desorption mass-transfer coefficients and for the four reaction rate constants, respectively. From the fitting results, the mass-transfer coefficient for adsorption ($k_{m,a}$) turned out not to be a function of temperature. It is not uncommon for

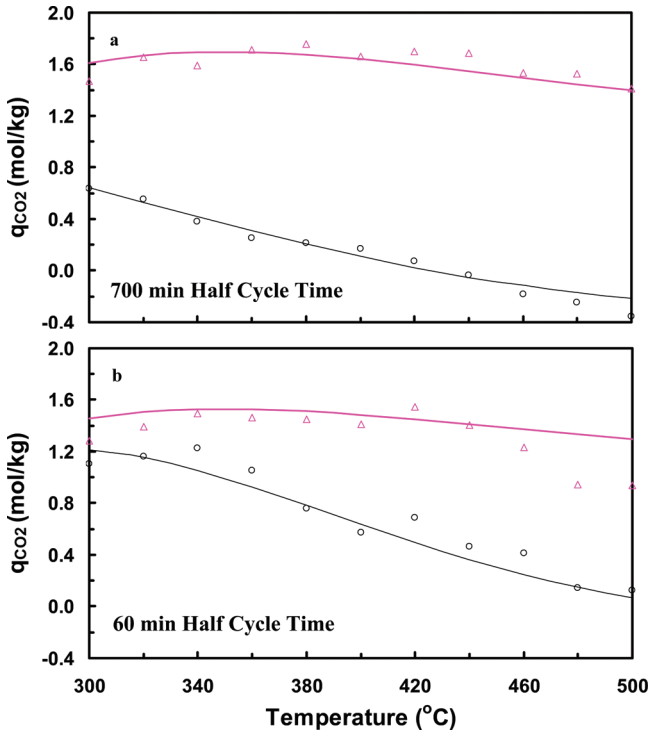

Figure 5. Experimental (symbols) and modeling (lines) results of the CO_2 loading in K-promoted HTlc as a function of temperature for (a) the CO_2 loading at the end of the adsorption (CO_2 at 1 atm) and desorption (He at 1 atm) steps during the 700 min half-cycle time shown in Figure 3 and (b) the CO_2 loading at the end of the eighth adsorption (CO_2 at 1 atm) and eighth desorption (He at 1 atm) steps during the 60 min half-cycle time shown in Figure 4.

Table 1. Temperature-Dependent RNEK Model Parameters That Describe the Adsorption and Desorption Behavior of CO_2 in K-Promoted HTlc from 300 to 500 °C

parameter		parameter	
	Known a Priori		
$q_{A,o}$, mol/kg	0.000	q_T, mol/kg	2.283
$q_{B,o}$, mol/kg	0.000	$\theta_{A,e,a}$	1.000
$q_{A,e,d}$, mol/kg	0.000		
	Fitted to Experiment		
$q_{C,o}$, mol/kg	0.625	$E_{1,b}$, kJ/mol	−46.208
$A_{m,a} = k_{m,a}$, min^{-1}	1.200	$A_{2,f}$, min^{-1}	1.699
$E_{m,a}$, kJ/mol	0.000	$E_{2,f}$, kJ/mol	27.815
$A_{m,d}$, min^{-1}	73.956	$A_{2,b}$, kg mol^{-1} s^{-1}	4.237×10^{-3}
$E_{m,d}$, kJ/mol	35.220	$E_{2,b}$, kJ/mol	−9.843
$A_{1,f} = k_{1,f}$, min^{-1}	2.750×10^{-4}	m	0.405
$E_{1,f}$, kJ/mol	0.000	n, K^{-1}	0.0103
$A_{1,b}$, kg mol^{-1} s^{-1}	2.691×10^{-7}	T_o, K	543.3387

a concentration-driven mass-transfer process to be independent of temperature or exhibit only a small temperature dependence.[18] In contrast, the mass-transfer coefficient for desorption ($k_{m,d}$) exhibited a strong temperature dependence with a positive activation energy, suggesting that these two fast rate processes associated with phase A were probably not the same phenomenon and that associated with desorption was a strongly activated diffusion process. This result perhaps begins to explain why $k_{m,d}$ is an order of magnitude smaller than $k_{m,a}$.

For both reactions,

$$A + B \xrightarrow{k_{1,b}} C \qquad (17a)$$

$$A + E \xrightarrow{k_{2,b}} B \qquad (17b)$$

Arrhenius relations were obtained for their forward rate constants. However, the resulting activation energy was negative, an unusual behavior that means the reaction rate decreases with increasing temperature. Although this is not very common, it has been explained in the literature as an apparent activation energy when both exothermic adsorption and reaction are occurring.[19−21] Indeed, exothermic adsorption followed by reaction are probably occurring during the formation of both phases B and C. In this situation, it is not uncommon to have the magnitude of the heat of adsorption (a negative quantity) exceed the magnitude of the activation energy (a positive quantity), which results in a negative apparent activation energy.[19,20]

For the reverse of these two processes, i.e.,

$$C \xrightarrow{k_{1,f}} A + B \qquad (18a)$$

$$B \xrightarrow{k_{2,f}} A + E \qquad (18b)$$

the former exhibited no temperature dependence and the later exhibited a positive apparent activation energy. In the first case, the magnitudes of the heat of adsorption and activation energy probably canceled each other, making this reaction temperature-independent. This result implies that the exothermic adsorption process aided in reducing the activation energy associated with the decomposition of phase C. A similar situation occurred for the second case, but, in this case, the decomposition of phase B was apparently dominated by the formation of an activated complex that required a large activation energy.

Model Validation with Short Cycle Time Experimental Data. The results in Figures 2b, 4, and 5b show the predictions from the RNEK model for the short cycle time experimental data for all the temperatures. These are true predictions from the model, because no adjustments were made to the parameters (Table 1) obtained from fitting the long cycle time data to it, as explained previously. Figure 2b shows that the model provided excellent predictions of the eight 120 min adsorption and desorption cycles at 400 °C. This was also true for most of the other temperatures, especially the first adsorption step, as shown in Figure 4. It also did very well in predicting the initial rates of adsorption and desorption at all temperatures and cycles. However, some deviations were observed, depending on the temperature and cycle number.

The model predicted the experimental data extremely well in the temperature range from 380 to 460 °C over all eight cycles. However, it began to exhibit some discrepancies outside this temperature range. For the lower temperatures, the CO_2 working capacity was predicted well but not the absolute CO_2 capacity. For the higher temperatures, the CO_2 working capacity was overpredicted by the model due to an over prediction of the CO_2 uptake, not the CO_2 loading at the end of desorption. In fact, a close comparison of the model predictions to the experiment at 480 and 500 °C revealed that the experimental CO_2 adsorption capacity began to decrease as early as the second cycle. This decrease could not be predicted by the model and was perhaps due to irreversible losses at these temperatures, as alluded to earlier. Because this simple model could not be expected to predict such losses, these discrepancies were considered to be inconsequential.

Figure 5b shows this overprediction of the CO_2 working capacity at the two highest temperatures where the experimental CO_2 capacity dropped off at the end of the adsorption step of the eighth cycle. Nevertheless, the model did very well in predicting the CO_2 working capacity at the other temperatures during this cycle. Because of this apparent irreversible loss of the experimental CO_2 capacity at the end of the adsorption step,

the experimental CO_2 working capacity exhibited a maximum in the temperature range of 400−440 °C, whereas that predicted from the model kept increasing with increasing temperature. As mentioned earlier, it was not possible for the model to predict such irreversible losses. Nevertheless, both the model and the experiments showed that the CO_2 working capacity decreased significantly to very small values as the temperature decreased from 400 to 300 °C. These results further substantiated that the optimum temperature range is between 380 and 440 °C for using K-promoted HTlc with CO_2 in a cyclic process.

Conclusions

A temperature-dependent, reversible nonequilibrium kinetic (RNEK) model that describes the adsorption and desorption behavior of CO_2 in a K-promoted hydrotalcite-like compound (HTlc) was developed. This model involves a three-step, four-phase process that reversibly undergoes adsorption or reaction with CO_2 in the K-promoted HTlc structure. It contains 21 parameters, 5 of which were known a priori. The remaining 16 parameters were obtained by fitting the model to experimental adsorption and desorption cycling data obtained from an in-house-synthesized K-promoted HTlc material.

This fitting exercise was done with a single adsorption (in CO_2 at 1 atm) and desorption (in He at 1 atm) cycle with a 700 min half-cycle time for 11 different temperatures ranging from 300 to 500 °C in 20 °C increments. This long cycle time was used to ensure that the experimental data approached an equilibrium state and covered all three kinetic regimes (i.e., the slow, intermediate, and fast regimes) associated with the uptake and release of CO_2 according to the three-step, four-phase process. The model correlated very well with this long cycle time experimental data, capturing all three kinetic regimes, the absolute CO_2 capacity, the CO_2 working capacity, and their temperature dependence.

The model was then used to predict similar shorter cycle time experiments using the same set of parameters. These adsorption and desorption cycling experiments were carried out with a 60 min half-cycle time for eight cycles at each temperature. This short cycle time was used to test the model under more realistic cycle times that might be used in a cyclic process. In this case, the model predictions of these short cycle time experiments were very good, capturing the kinetics, the absolute CO_2 capacity, the periodic behavior during cycling, the CO_2 working capacity, and their temperature dependence. Although some deviations between the model and experiments were observed for both long and short cycle times, they were mostly due to slight irreversible losses in the CO_2 capacity observed for the short cycle time runs in the 480−500 °C range that the model could not predict. These deviations were thus considered to be inconsequential.

In general, the model did very well in predicting the completely reversible adsorption and desorption behavior of CO_2 in K-promoted HTlc over a wide range of cycle times (120−1400 min) and temperatures (300−500 °C). Both the model and experiments showed that temperature played an important role, with higher temperatures generally improving the behavior and with optimum behavior occurring in the 380−420 °C temperature range. Overall, this new temperature-dependent RNEK model further validated that CO_2 uptake and release in K-promoted HTlc is associated with a combination of completely reversible adsorption, diffusion, and reaction phenomena, through a three-step, four-phase process that has a strong temperature dependence.

Acknowledgment

The authors gratefully acknowledge financial support provided by the Center for Clean Coal at the University of South Carolina, the DOE through Grant No. DE-FG26-03NT41799, and the Separations Research Program at the University of Texas at Austin.

Nomenclature

A = reaction site for weakly chemisorbed CO_2 in K-promoted HTlc
$A_{i,j}$ = preexponential factor in the Arrhenius-type relationships for the reaction and mass-transfer processes i = m, 1, 2; j = f, b
B = reaction site for one molecule of chemically bound CO_2 in K-promoted HTlc, i.e., $Mg_6Al_2K_2O_9(CO_3)$
C = reaction site for two molecules of chemically bound CO_2 in K-promoted HTlc, i.e., $Mg_6Al_2K_2O_8(CO_3)_2$
E = reaction site free of CO_2 in K-promoted HTlc, i.e., $Mg_6Al_2K_2O_{10}$
$E_{i,j}$ = activation energy in the Arrhenius type relationships for the reaction and mass-transfer processes i = m, 1, 2; j = f, b
$k_{1,f}$ = forward rate constant for reaction 18a (min^{-1})
$k_{1,b}$ = backward rate constant for reaction 18a ((kg/mol)/min)
$k_{2,f}$ = forward rate constant for reaction 18b (min^{-1})
$k_{2,b}$ = backward rate constant for reaction 18b ((kg/mol)/min)
$k_{m,a}$ = mass-transfer coefficient for adsorption of CO_2 from the gas phase into phase A (min^{-1})
$k_{m,d}$ = mass-transfer coefficient for desorption of CO_2 from phase A into the gas phase (min^{-1})
m = fitting parameter for η
n = fitting parameter for η
M_{CO_2} = molecular weight of CO_2 (kg/mol)
$q_{A,e}$ = concentration of site A at equilibrium (mol of sites/(kg of CO_2-free K-promoted HTlc))
$q_{A,e,a}$ = concentration of site A at equilibrium after adsorption (mol of sites/(kg of CO_2-free K-promoted HTlc))
$q_{A,max}$ = maximum concentration of site A formed during adsorption (mol of sites/(kg of CO_2-free K-promoted HTlc))
$q_{A,e,d}$ = concentration of site A at equilibrium after desorption (mol of sites/(kg of CO_2-free K-promoted HTlc))
q_{CO_2} = CO_2 loading relative to q_o (mol of CO_2/(kg of CO_2-free K-promoted HTlc))
q_o = CO_2 loading after activation (mol of CO_2/(kg of CO_2-free K-promoted HTlc))
q_T = total number of reaction sites available for chemically bound CO_2 (mol of sites/(kg of CO_2-free K-promoted HTlc))
q_X = concentration of site X, with X = A, B, C, or E (mol of sites/(kg of CO_2-free K-promoted HTlc))
$q_{X,o}$ = concentration of site X after activation, with X = A, B, C, or E (mol of sites/(kg of CO_2-free K-promoted HTlc))
T_o = fitting parameter for η
w = experimental mass (g)
w_o = experimental mass just after activation (g)

Greek Letters

$\theta_{A,e,a}$ = fractional coverage of phase A at equilibrium
η = ratio of actual reaction sites to the maximum number of reaction sites

Literature Cited

(1) Nataraj, S.; Carvill, B. T.; Hufton, J. R.; Mayorga, S. G.; Gaffney, T. R.; Brzozowski, J. R. Process for Operating Equilibrium Controlled Reactions. *Can. Patent* **1998**, 2,235,928.

(2) Ding, Y.; Alpay, E. Equilibria and Kinetics of CO_2 Adsorption on Hydrotalcite Adsorbent. *Chem. Eng. Sci.* **2000**, *55*, 3461.

(3) Yong, Z.; Mata, V.; Rodrigues, A. E. Adsorption of Carbon Dioxide onto Hydrotalcite-like Compounds (HTlcs) at High Temperature. *Ind. Eng. Chem. Res.* **2001**, *40*, 204.

(4) Hufton, J. R.; Mayorga, S.; Sircar, S. Sorption-Enhanced Reaction Process for Hydrogen Production. *AIChE J.* **1999**, *45*, 248.

(5) Ding, Y.; Alpay, E. Adsorption-Enhanced Steam-Methane Reforming. *Chem. Eng. Sci.* **2000**, *55*, 3929.

(6) Reijers, H.; Th., J.; Valster-Schiermeier, S. A. E.; Cobden, P. D.; van den Brink, R. Hydrotalcite as CO_2 Sorbent for Sorption-Enhanced Steam Reforming of Methane. *Ind. Eng. Chem. Res.* **2006**, *45*, 2522.

(7) van Selow, E. R.; Cobden, P. D.; Verbraeken, P. A.; Hufton, J. R.; van den Brink, R. W. Carbon Capture by Sorption-Enhanced Water-Gas Shift Reaction Process using Hydrotalcite-Based Material. *Ind. Eng. Chem. Res.* **2009**, *48*, 4184.

(8) Reijers, H.; Th., J.; Boon, J.; Elzinga, G. D.; Cobden, P. D.; Haije, W. G.; van den Brink, R. W. Modeling Study of the Sorption-Enhanced Reaction Process for CO_2 Capture. I. Model Development and Validation. *Ind. Eng. Chem. Res.* **2009**, *48*, 6966.

(9) Reijers, H.; Th., J.; Boon, J.; Elzinga, G. D.; Cobden, P. D.; Haije, W. G.; van den Brink, R. W. Modeling Study of the Sorption-Enhanced Reaction Process for CO_2 Capture. II. Application to Steam-Methane Reforming. *Ind. Eng. Chem. Res.* **2009**, *48*, 6975.

(10) Reynolds, S. P.; Ebner, A. D.; Ritter, J. A. New Pressure Swing Adsorption Cycles for Carbon Dioxide Sequestration. *Adsorption* **2005**, *11*, 531.

(11) Reynolds, S. P.; Ebner, A. D.; Ritter, J. A. Stripping PSA Cycles for CO_2 Recovery from Flue Gas at High Temperature Using a Hydrotalcite-like Adsorbent. *Ind. Eng. Chem. Res.* **2006**, 4278.

(12) Reynolds, S. P.; Mehrotra, A.; Ebner, A. D.; Ritter, J. A. Heavy Reflux PSA Cycles for CO_2 Recovery from Flue Gas: Part I. Performance Evaluation. *Adsorption* **2008**, *14*, 399.

(13) Moreira, R. F. P. M.; Soares, J. L.; Casarin, G. L.; Rodrigues, A. E. Adsorption of CO_2 on Hydrotalcite-like Compounds in a Fixed Bed. *Sep. Sci. Technol.* **2006**, *41*, 341.

(14) Lee, K. B.; Verdooren, A.; Caram, H. S.; Sircar, S. Chemisorption of Carbon Dioxide on Potassium-Carbonate-Promoted Hydrotalcite. *J. Colloid Interface Sci.* **2007**, *308*, 30.

(15) Oliverira, E. L. G.; Grande, C. A.; Rodrigues, A. E. CO_2 Sorption on Hydrotalcite and Alkali-Modified (K and Cs) Hydrotalcite at High Temperatures. *Sep. Purif. Technol.* **2008**, *62*, 137.

(16) Ebner, A. D.; Reynolds, S. P.; Ritter, J. A. Understanding the Adsorption and Desorption Behavior of CO_2 on a K-Promoted HTlc through Non-equilibrium Dynamic Isotherms. *Ind. Eng. Chem. Res.* **2006**, *45*, 6387.

(17) Ebner, A. D.; Reynolds, S. P.; Ritter, J. A. Nonequilibrium Kinetic Model That Describes the Reversible Adsorption and Desorption Behavior of CO_2 in a K-Promoted Hydrotalcite-like Compound. *Ind. Eng. Chem. Res.* **2007**, *46*, 1737.

(18) Al-Muhtaseb, S. A.; Ritter, J. A. New Methodology for the Measurement and Analysis of Adsorption Dynamics: Butane on Activated Carbon. *Ind. Eng. Chem. Res.* **2004**, *43*, 7075.

(19) Davis, M. E. Davis, R. J. *Fundamentals of Chemical Reaction Engineering*; McGraw-Hill: New York, 2003.

(20) Wei, J. Adsorption and Cracking of N-Alkanes over ZSM-5: Negative Activation Energy of Reaction. *Chem. Eng. Sci.* **1996**, *51*, 2995.

(21) Chorkendorff, I.; Niemantsverdriet, J. W. *Concepts of Modern Catalysis and Kinetics*; Wiley-VCH: New York, 2003.

Received for review July 31, 2009
Revised manuscript received January 27, 2010
Accepted February 4, 2010

IE901210Y